

# THE GRAVITATIONAL LENS – GALAXY GROUP CONNECTION. II. GROUPS ASSOCIATED WITH B2319+051 AND B1600+434

M. W. AUGER, C. D. FASSNACHT, A. L. ABRAHAMSE, L. M. LUBIN  
 Department of Physics, University of California, 1 Shields Avenue, Davis, CA 95616

G. K. SQUIRES

Spitzer Science Center, California Institute of Technology, Mail Code 220-6, 1200 E. California Blvd., Pasadena, CA 91125  
*Submitted to AJ*

## ABSTRACT

We report on the results of a spectroscopic survey of the environments of the gravitational lens systems CLASS B1600+434 ( $z_l = 0.41, z_s = 1.59$ ) and CLASS B2319+051 ( $z_l = 0.62$ ). The B1600+434 system has a time delay measured for it, and we find the system to lie in a group with a velocity dispersion of  $100 \text{ km s}^{-1}$  and at least six members. B2319+051 has a large group in its immediate foreground with at least 10 members and a velocity dispersion of  $460 \text{ km s}^{-1}$  and another in the background of the lens with a velocity dispersion of  $190 \text{ km s}^{-1}$ . There are several other small groups in the fields of these lens systems, and we describe the properties of these moderate redshift groups. Furthermore, we quantify the effects of these group structures on the gravitational lenses and find a  $\sim 5\%$  correction to the derived value of  $H_0$  for B1600+434.

*Subject headings:* distance scale — galaxies: individual (B2319+051, B1600+434) — gravitational lensing – galaxies: groups

## 1. INTRODUCTION

Galaxy groups are a fundamental component of the Large Scale Structure of the Universe and over half of all galaxies in the local Universe are members of groups (e.g., Tully 1987; Ramella et al. 1989). Precision cosmology relies on an accurate knowledge of the distribution of galaxies in order to model the galaxy power spectrum properly (e.g., Evrard et al. 2002; Yang et al. 2004), and it is essential that galaxy groups are identified to describe the small-scale, non-linear regime of the matter power spectrum accurately. Several local redshift surveys, including the Sloan Digital Sky Survey (SDSS, York et al. 2000) and the 2 Degree Field Galaxy Redshift Survey (2dFGRS, Colless et al. 2001), have produced results using groups out to  $z \sim 0.2$  (Weinmann et al. 2006; Collister & Lahav 2005; Abazajian et al. 2005; Padilla et al. 2004). At higher redshifts, the Canadian Network for Observational Cosmology redshift survey (CNOC2, Carlberg et al. 2001a) probes redshifts  $0.15 \lesssim z \lesssim 0.5$ , while the DEEP2 Galaxy Redshift Survey is probing redshifts from  $0.7 \lesssim z \lesssim 1$  (Coil et al. 2006, 2004). Weak lensing analyses of groups also promise to yield information about the mass distribution in galaxy groups (e.g., Möller et al. 2002; Faure et al. 2004; Hoekstra et al. 2001). Knowledge of group substructure can then be used to confirm or refute dark matter models (Reed et al. 2005; D’Onghia & Lake 2004).

Groups also hold significance for strong gravitational lensing. Keeton et al. (2000) estimate that 25% of lenses lie in group environments, though the fraction could be much higher (e.g., Williams et al. 2005; Blandford et al. 2001; Oguri et al. 2005). A moderately massive group that is sufficiently close to the lensing galaxy can contribute to the convergence in the lensing potential and alter the shear field of the lens. Theoretical esti-

mates of the importance of these contributions have been made (e.g., Oguri et al. 2005; Keeton & Zabludoff 2004; Möller et al. 2002) but it remains unclear to what extent lens models must account for group environments (e.g., Momcheva et al. 2005; Fassnacht et al. 2005; Morgan et al. 2005; Dalal & Watson 2004). Furthermore, gravitational lens time-delay measurements and improved mass modeling techniques have lowered the uncertainties in measurements of the Hubble Constant,  $H_0$ , to the  $\approx 10\%$  level (e.g., Koopmans et al. 2003; Kochanek & Schechter 2004), and the systematic errors introduced by ignoring lens environments now contribute significantly to the  $H_0$  error budget.

In addition to improving the determination of cosmological parameters, galaxy groups also allow us to study the evolution of galaxies. Group environments are likely locations for mergers (e.g., Zabludoff & Mulchaey 1998; Carlberg et al. 2001b; Aarseth & Fall 1980) compared to clusters or the field (e.g., Aceves & Velázquez 2002; Lin et al. 2004; Conselice et al. 2003; Patton et al. 2002). Mergers and non-merger interactions in groups can drive changes in galaxy morphologies and star formation rates (SFR) that are suppressed in more dense environments (e.g., Zabludoff & Mulchaey 1998; Bower & Balogh 2004). Furthermore, active galactic nuclei (AGN) are expected to reside in dense environments where galaxy-galaxy interactions provide mechanisms for fueling AGN (e.g., Best 2004; Bahcall et al. 1997), though the validity of this claim is uncertain (e.g., Kauffmann et al. 2004; Miller et al. 2003). Best et al. (2005) only find a correlation between *radio-loud* AGN and the local environment, although McLure & Dunlop (2001) find no distinction between radio-loud and radio-quiet AGN populations in clusters.

We are currently conducting a systematic survey to investigate the environments of strong gravitational lens systems (e.g., Fassnacht & Lubin 2002;

Fassnacht et al. 2005). In this paper we present the discovery of three groups associated with the lens systems B1600+434 (Jackson et al. 1995) and B2319+051 (Rusin et al. 2001), hereafter B1600 and B2319. These lenses were discovered by the Cosmic Lens All-Sky Survey (CLASS; Myers et al. 2003; Browne et al. 2003). In the case of B2319, the lens is not found to be part of a group, but there is a large group in the immediate foreground of the lens and another group in the background of the lens. In contrast, B1600 is found to be a member of a poor group of galaxies. Here we examine the effects of these new groups on the lens models for each system, quantifying the contributions of the environments to the shears and convergences of the lens systems. The final sample of groups from our study will be compared with groups observed in the local Universe (Merchán & Zandivarez 2005; Balogh et al. 2004) and with recent observations of other moderate redshift groups (Wilman et al. 2005a,b; Momcheva et al. 2005; Williams et al. 2005; Gerke et al. 2005) to quantify the evolution of groups with redshift.

## 2. OBSERVATIONS AND DATA REDUCTION

There are approximately 80 known strong gravitational lens systems, and many of these require only very small *ad hoc* additional shear and convergence components to be adequately modeled (e.g., Lehar et al. 2000). In contrast, the B2319 system ( $z_l = 0.62$ ) requires a large shear component to fit acceptable models, and this shear cannot be entirely accounted for by the lensing galaxy (Rusin et al. 2001). There is a secondary lensing candidate  $3''.4$  away from the primary lens, and the redshifts of the lensing and secondary galaxies are 0.624 and 0.588, respectively (Lubin et al. 2000). However, it is likely that the secondary galaxy alone cannot account for the shear discrepancy, and a more massive, group-like structure is required to reproduce the observed image configuration. The B1600 system ( $z_l = 0.41, z_s = 1.59$ ) has a reasonably well constrained lens model (Koopmans et al. 1998; Maller et al. 2000), but initial spectroscopy of the environment of the lensing galaxy has revealed several nearby galaxies with redshifts similar to the lensing galaxy. It is crucial that the group associated with B1600 be investigated due to the importance of this system in determining  $H_0$  (Koopmans et al. 2000; Maller et al. 2000; Kochanek 2002, 2003; Burud et al. 2000).

### 2.1. Imaging

We have obtained deep non-photometric BVRI images of B2319 using the Low-Resolution Imaging Spectrometer (LRIS; Oke et al. 1995) and Echelle Spectrograph and Imager (ESI; Sheinis et al. 2002) instruments on the Keck Telescopes. We have also obtained photometric LRIS snapshots of the field in the BVI filters, allowing us to photometrically calibrate our deeper imaging in these bands. These Keck imaging data were reduced using standard IRAF<sup>1</sup> tasks. Our primary imaging of B1600 comes from deep BRI imaging from the Suprime-Cam instrument (Miyazaki et al. 2002) on the Subaru Telescope, obtained from the SMOKA archive (Baba et al.

2002). These data were reduced using the SDFRED package (Ouchi et al. 2004). A comparison between stars in our Suprime-Cam imaging and SDSS imaging of the field of B1600 (after applying Lupton's transformation<sup>2</sup> between the two different filter sets) allowed us to establish a photometric zeropoint for the Suprime-Cam archival data. Additionally, we have *Hubble Space Telescope* (HST) imaging of both fields with the WFPC2 camera in the F555W and F814W filters. A summary of our imaging data can be found in Table 1.

### 2.2. Spectroscopy

The candidate group members for the two lens systems were chosen based upon the colors of the lensing galaxy or other galaxies in the field at the same redshift as the lens. Target galaxies generally had colors within 0.1 mag of the colors of the lensing galaxy and were within  $200''$  of the lensing galaxy. Four slitmasks were taken for the field of B2319 and one slitmask was obtained for the field of B1600 with LRIS (Table 2). A handful of additional redshifts were also obtained from longslit spectra of each lens system with LRIS and ESI. The spectra were reduced using standard IRAF tasks, and redshifts were determined by finding at least one emission line and one other feature, or by identifying multiple absorption features in each spectrum. Redshift errors are typically  $\Delta z \approx 0.0004$ . In total, we have 53 redshifts for the B2319 field and 24 redshifts for the B1600 field (the number of redshifts in Table 2 does not reflect our longslit spectra but do include multiple observations of some target galaxies; all five targets with repeated observations have redshifts that agree within the measurement errors).

## 3. GROUP IDENTIFICATION

The redshift distributions obtained from the spectroscopy of our two target lens systems are shown in Figures 1 and 2. There are two obvious peaks in the field of B2319 and one clear peak at the lens redshift of B1600. We identify possible groups by initially associating all galaxies that are within  $\delta z = 0.005$  of each other (in effect, we take each spike from the redshift distribution to be a potential group). We then use the formalism of Wilman et al. (2005a) to exclude non-members and to determine the group's velocity dispersion. That is, we find the average redshift and position of the potential group members (clipping the extreme members for groups with more than 3 potential members), define a first approximation observed velocity dispersion of  $\sigma_{obs} = 350 (1 + \bar{z}) \text{ km s}^{-1}$ , set an initial redshift shell

$$\delta z = \frac{2 \sigma_{obs}}{c},$$

and specify a maximum angular radius based upon this redshift shell (see Wilman et al. 2005a, for example):

$$\delta \theta = 206265'' \frac{c \delta z}{b(1 + \bar{z}) H_0 D_\theta}.$$

Here,  $D_\theta$  is the angular diameter distance at the mean redshift. We will assume a  $\Lambda$ CDM cosmology with  $\Omega_m =$

<sup>1</sup> IRAF is distributed by the National Optical Astronomy Observatories, which are operated by the Association of Universities for Research in Astronomy, Inc., under cooperative agreement with the National Science Foundation.

<sup>2</sup> We used the filter transformations that had smaller reported values for sigma. Lupton's filter transformation equations can be found on the SDSS Data Release 4 website at: <http://www.sdss.org/dr4/algorithms/sdssUBVRITransform.html>

TABLE 1  
LENS SYSTEM IMAGING

Lens System	Band	Exposure Time (s)	Instrument	Date
B2319+051	R	1200	LRIS	1998 Aug 01
	B	900	LRIS	1999 Aug 16
	V	3900	LRIS	1999 Aug 16
	I	2700	LRIS	1999 Aug 16
	F555W	4800	WFPC2	2000 Sep 27
	F814W	4800	WFPC2	2000 Sep 27
B1600+434	B	1200	Suprime-Cam	2001 May 21
	R	2700	Suprime-Cam	2001 Apr 25,26
	I	1380	Suprime-Cam	2001 Apr 20
	F555W	5300	WFPC2	2001 Jun 16
	F555W	18200	WFPC2	2001 Sep 21-23
	F814W	7800	WFPC2	2001 Sep 26

TABLE 2  
LENS FIELD LRIS SPECTROSCOPY

Lens System	Number of Redshifts	Exposure Time (s)	Date
B2319+051	8	5400	2001 Jul 26
	21	8100	2002 Jul 15
	12	3600	2002 Jul 16
	15	5400	2003 Aug 01
B1600+434	21	5400	2003 Jul 31

0.27 and  $\Omega_\Lambda = 0.73$ , and we follow Wilman et al. (2005a) in fixing our aspect ratio,  $b = 3.5$ .

Upon excluding potential members outside of our redshift shell  $\delta z$  and our maximum radius  $\delta\theta$ , we compute the velocity dispersion of the remaining group members. We calculate  $\sigma_{obs}$  using the standard deviation, the gapper algorithm, and a clipped standard deviation. Each of these methods resulted in the same group membership, and we report the results obtained from the gapper algorithm to allow direct comparison with the Wilman et al. (2005a) sample. We use the updated value for  $\sigma_{obs}$  to determine a new  $\delta z$  and  $\delta\theta$  and repeat the process until no more potential members are eliminated; for each potential group, stable membership was achieved in two iterations.

We retain any associations with three or more members. This leaves us with three groups in the field of B1600 and four groups in the field of B2319. The details for these groups are listed in Table 3 and the velocity distribution of each group containing six or more members is shown in Figure 3. Errors in the velocity dispersion were determined using a jackknife analysis; errors for groups with 3 members are not meaningful. The group located at  $z = 0.5894$  in the field of B2319 could be two smaller groups interacting, as indicated by the bimodal velocity distribution, or it could be a small cluster. Until we obtain more redshift information for the field, we will treat it as a single group.

#### 4. GROUP PROPERTIES

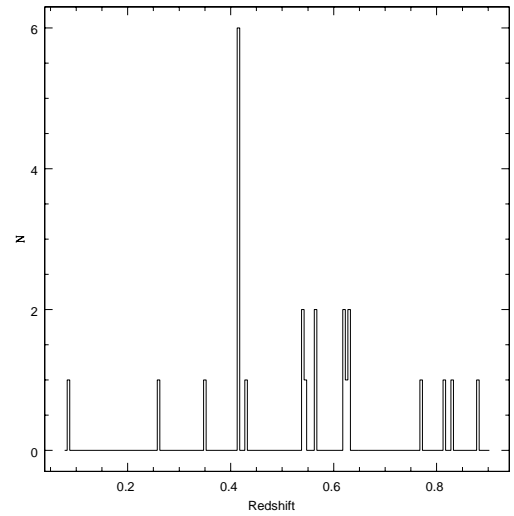


FIG. 1.— Redshift distribution of galaxies in the field of the gravitational lens B1600+434. The redshift of the lens is 0.41.

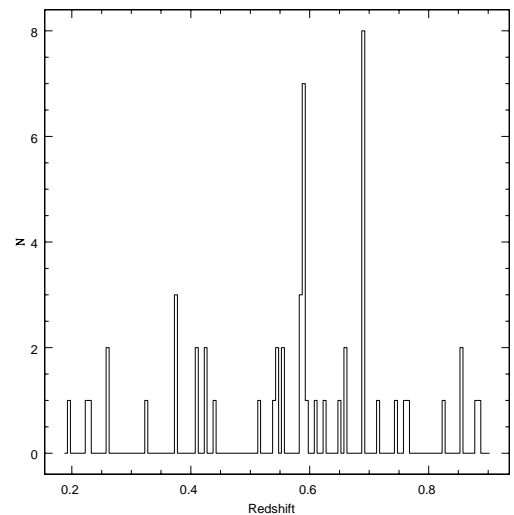


FIG. 2.— Redshift distribution of field galaxies for the gravitational lens B2319+051. The redshift of the lens is 0.62.

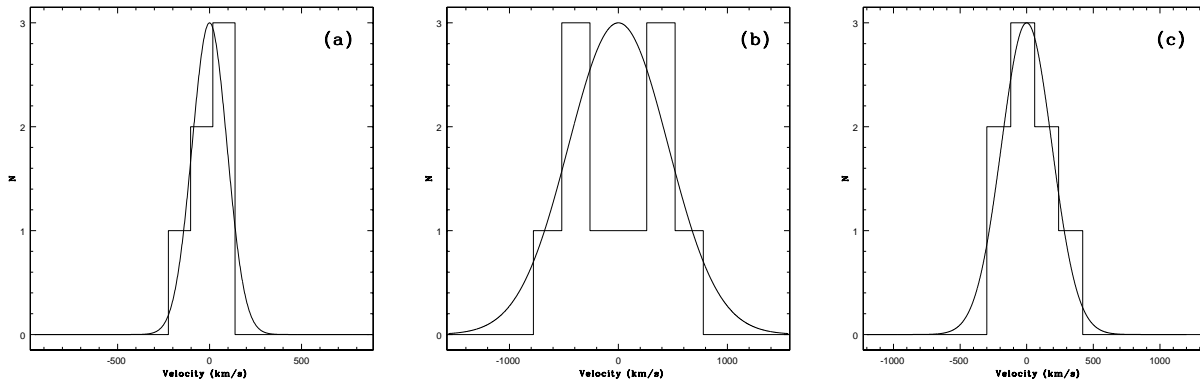


FIG. 3.— Velocity histograms for members of the groups associated with (a) B1600+434 and the (b) foreground and (c) background groups of B2319+051.

As outlined in Table 3, we have detected three larger groups with six or more members and four smaller groups. Whether many of these smaller groups are bound systems is questionable. For example, the two small groups associated with B1600+434 have significantly larger velocity dispersions than typical small groups (e.g., Merchán & Zandivarez 2005). We report parameters for these small groups, but we limit our discussion to the three groups with more than five members. The velocity dispersions of these groups are consistent with other groups with comparable numbers of members (Wilman et al. 2005a). In determining group parameters, we have assumed that the groups are relaxed and we use the virial theorem to determine masses and radii.

We are hesitant to quote group properties due to the incompleteness of our group member sampling. Nevertheless, we provide estimates for the virial radius, mean pairwise separation, mass, and crossing time for each group; the values listed in Table 3 for these properties should be considered order of magnitude estimates. Following the definitions of Ramella et al. (1989), we define the group’s virial radius

$$R_{vir} = \frac{\pi}{2} D_{\theta} N_{pairs} \left( \sum_i \sum_{j>i} \theta_{ij}^{-1} \right)^{-1},$$

the mean (physical) separation between pairs

$$R_p = \frac{4}{\pi} D_{\theta} N_{pairs}^{-1} \sum_i \sum_{j>i} \theta_{ij},$$

the virial mass

$$M_{vir} = \frac{6\sigma^2 R_{vir}}{G},$$

and the crossing time

$$t_c = \frac{3R_{vir}H_0}{5^{3/2}\sigma}$$

where  $D_{\theta}$  is the angular diameter distance at the group’s redshift,  $N_{pairs} = N_{mem}(N_{mem} - 1)/2$  is the number of unique group member pairs,  $\theta_{ij}$  is the angular separation between group members, and  $t_c$  is measured in Hubble times.

*HST* imaging is used to determine morphological classifications of group members that lie within the WFPC2 field of view (Figure 4), which includes most galaxies within  $\sim 90''$  of the lensing galaxy. Additionally, we indicate whether the group galaxies have strong emission lines present in their spectra. Considering the nature of the morphological and spectral features for each galaxy, we characterize the galaxies as either late-(spiral/irregular morphologies or strong emission features and poor morphological information) or early-type galaxies (early-type or uncertain morphologies and no emission features).

We find that all of the galaxies that we associate with B1600 are late-type galaxies (see Table 4). With a velocity dispersion of  $\approx 100 \text{ km s}^{-1}$  and only six members, this early-type fraction of zero is similar to some of the results of Zabludoff & Mulchaey (1998), who found that groups with no early type galaxies had lower velocity dispersions and fewer members than groups with non-zero early-type fractions. Dai & Kochanek (2005) do not find any X-ray emission associated with the B1600 group, which is also expected for groups with low velocity dispersions and low early-type fractions (e.g., Zabludoff & Mulchaey 1998; Mulchaey et al. 2003). The absence of X-ray emission indicates that the group may not be relaxed, in which case the mass reported for the group is not valid.

The groups associated with B2319 have more varied populations than the B1600 group (see Tables 5 and 6). Using our characterization scheme, the early-type fractions for these groups are 0.5 and 0.63 for the foreground and background groups. These early-type fractions are typical of groups in the local Universe that tend to also have X-ray emission associated with them (Zabludoff & Mulchaey 1998; Mulchaey et al. 2003), although B2319 has not yet been observed at X-ray wavelengths. These early-type fractions lead us to believe that these two groups are likely to be bound and relaxed structures, and therefore the mass estimates derived from the measured velocity dispersions approximate the masses of these groups.

In Figure 5 we plot the locations of the early-type (circles) and late-type (squares) galaxies in each group with respect to the group center. Each field is  $2 h^{-1} \text{ Mpc}$  on a side and the central circle has a radius of  $0.5 h^{-1} \text{ Mpc}$ .

TABLE 3  
SUMMARY OF GALAXY GROUPS IN THE FIELDS OF B1600 AND B2319

Field	RA	Dec	$z$	$N_{mem}$	$\sigma$ (km s $^{-1}$ )	$M_{vir}$ ( $10^{14} h M_{\odot}$ )	$R_{vir}$ ( $h^{-1}$ Mpc)	$R_p$ ( $h^{-1}$ Mpc)	$t_c$ (Hubble times)
B1600	16 01 40	43 16 48	0.415	6	$100 \pm 40$	0.19	0.16	0.33	0.04
	16 01 40	43 17 44	0.543	3	$640 \pm 770$	7.25	1.02	0.93	0.04
	16 01 39	43 17 09	0.629	5	$840 \pm 350$	9.6	1.02	0.99	0.03
B2319	23 21 39	05 26 52	0.589	10	$460 \pm 80$	0.67	0.24	0.42	0.01
	23 21 40	05 26 48	0.689	8	$190 \pm 50$	0.15	0.32	0.41	0.05
	23 21 41	05 27 43	0.375	3	$340 \pm 240$	0.64	0.43	0.62	0.03
	23 21 40	05 26 21	0.542	3	$260 \pm 290$	1.03	1.10	1.16	0.11

TABLE 4  
MEMBERS OF B1600 GROUP

Label	RA	Dec	$z$	B <sup>a</sup>	R <sup>a</sup>	I <sup>a</sup>	Morphology <sup>b</sup>	Emission
1600_1_1	16 01 40.48	43 16 48.0	0.4144	21.50	19.91	19.22	Sa	Yes
1600_1_2	16 01 40.84	43 16 45.2	0.4146	21.84	19.61	18.87	SBa	Yes
1600_1_3	16 01 39.58	43 16 48.3	0.4151	23.60	21.39	20.54	Sc	Yes
1600_1_4	16 01 42.83	43 17 01.1	0.4140	23.60	21.96	21.53	Sd	Yes
1600_1_5	16 01 41.83	43 18 03.6	0.4149	25.36	24.04	23.76	Irr	Yes
1600_1_6	16 01 36.16	43 15 23.2	0.4150	23.32	21.78	21.35	Irr	Yes

<sup>a</sup>From Subura Suprime-Cam imaging

<sup>b</sup>Determined from WFPC2 F555W and F814W imaging

TABLE 5  
MEMBERS OF B2319 FOREGROUND GROUP

Label	RA	Dec	$z$	B <sup>a</sup>	V <sup>a</sup>	I <sup>a</sup>	Morphology <sup>b</sup>	Emission
2319_1_1	23 21 37.25	05 25 09.2	0.5867	24.28	23.61	21.85	...	Yes
2319_1_2	23 21 43.37	05 25 43.9	0.5868	24.47	23.01	20.70	...	No
2319_1_3	23 21 37.54	05 26 22.1	0.5893	23.27	22.39	20.39	Irr	Yes
2319_1_4	23 21 38.24	05 27 11.3	0.5861	23.96	22.09	19.59	E	No
2319_1_5	23 21 39.39	05 27 19.2	0.5917	26.12	23.94	21.51	E	Yes
2319_1_6	23 21 40.73	05 27 23.9	0.5922	24.24	23.94	22.75	Irr	Yes
2319_1_7	23 21 38.23	05 27 38.3	0.5913	23.27	21.70	19.11	E	No
2319_1_8	23 21 38.41	05 27 33.2	0.5876	24.97	23.12	20.45	E	No
2319_1_9	23 21 38.82	05 27 31.5	0.5910	25.73	24.47	22.31	Sa	No
2319_1_10	23 21 40.61	05 27 38.2	0.5888	25.08	23.55	21.11	Irr	Yes

<sup>a</sup>From Keck LRIS imaging

<sup>b</sup>Determined from WFPC2 F555W and F814W imaging when available

TABLE 6  
MEMBERS OF B2319 BACKGROUND GROUP

Label	RA	Dec	$z$	B <sup>a</sup>	R <sup>a</sup>	I <sup>a</sup>	Morphology <sup>b</sup>	Emission
2319_2_1	23 21 37.17	05 25 57.2	0.6887	25.95	24.72	22.13	...	No
2319_2_2	23 21 39.98	05 26 07.8	0.6891	23.97	23.69	22.65	...	Yes
2319_2_3	23 21 40.65	05 26 27.7	0.6905	25.31	23.36	20.93	...	No
2319_2_4	23 21 41.99	05 26 40.0	0.6881	23.79 <sup>c</sup>	22.13 <sup>c</sup>	19.31 <sup>c</sup>	...	No
2319_2_5	23 21 41.99	05 26 40.0	0.6884	... <sup>c</sup>	... <sup>c</sup>	... <sup>c</sup>	...	No
2319_2_6	23 21 43.02	05 26 48.7	0.6879	25.87	24.43	21.71	...	No
2319_2_7	23 21 41.97	05 26 56.4	0.6903	25.05	24.45	22.82	...	Yes
2319_2_8	23 21 39.16	05 28 29.3	0.6898	24.08	23.55	21.92	S0	Yes

<sup>a</sup>From Keck LRIS imaging

<sup>b</sup>Determined from WFPC2 F555W and F814W imaging when available

<sup>c</sup>We are not able to extract individual magnitudes for these objects from our imaging data; however, the objects have distinct spectral traces, so we report them as individual galaxies

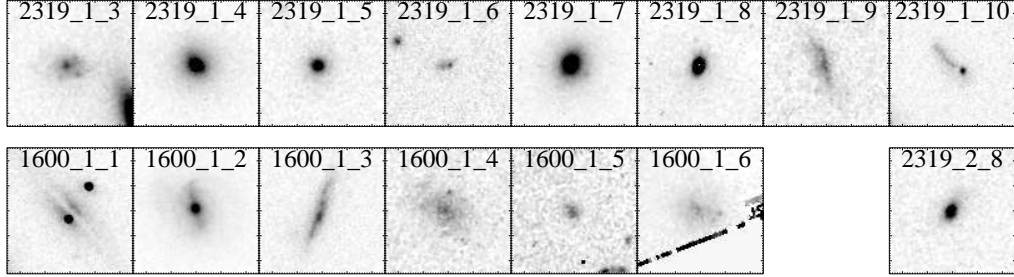


FIG. 4.— HST WFPC2 imaging of the B1600 and B2319 lens systems; each image is  $5''.05$  on a side. The images for 1600\_1\_4 and 1600\_1\_5 are taken from the F555W filter, and the rest of the images are from the F814W filter. The lens in B1600 is 1600\_1\_1.

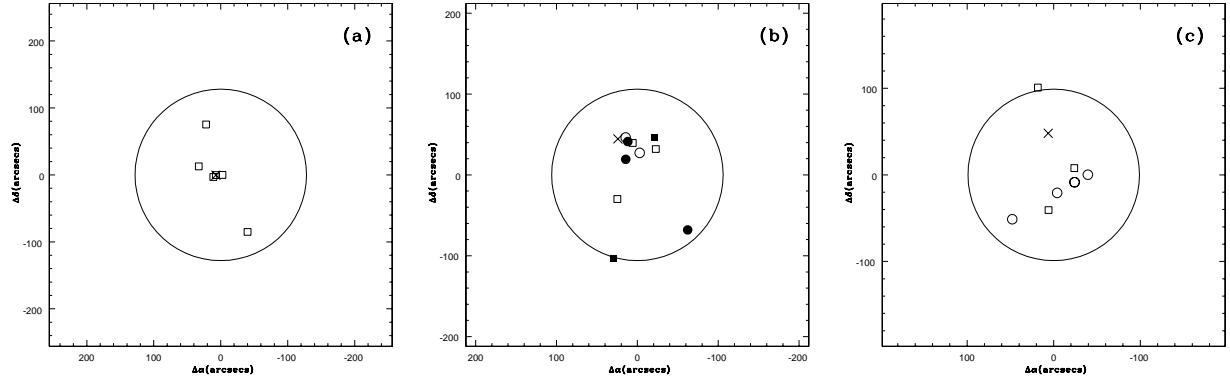


FIG. 5.— Spatial distribution of early-type (circles) and late-type (squares) galaxies for the (a) B1600 group and the (b) foreground and (c) background groups of B2319. The fields are centered on the group center and are  $2 h^{-1}\text{Mpc}$  on a side. The central circle has a radius of  $0.5 h^{-1}\text{Mpc}$ , and the X marks the position of the lensing galaxy. Late-type galaxies are marked with squares and early-types with circles. The shaded markers in (b) represent galaxies with negative velocities in the bimodal velocity distribution of Figure 3b and the open markers are galaxies with positive velocities.

We also show the location of the lensing galaxy, denoted by an X, with respect to the group centers. For the B2319 foreground group, we mark the galaxies with positive velocities (see Figure 3b) with open symbols and galaxies with negative velocities with filled symbols.

The center of the B1600 group is coincident with the lensing galaxy, although the overall structure of the group is somewhat filamentary. This elongated structure could be due to only having one slitmask for the group, causing a bias in the selection of target galaxies; the group is roughly aligned along the North-South axis, which is also the orientation axis of the slitmask. The distribution of the inner four galaxies of the group is very compact, and the group meets all of the criteria of Hickson (1982) for compact groups except the requirement that the group be isolated from other galaxies (to distinguish compact groups from cluster- or in this case group-cores, for example).

We find that neither of the groups associated with B2319 are centered on the lensing galaxy. The background group has an elongated structure similar to the B1600 group, although this B2319 group is not preferentially aligned with the slitmasks used for the field. The B2319 groups do not show a preference for early-type galaxies lying in the center of the groups, contrary to what one might expect for relaxed groups. However, the foreground group appears to be quite compact with seven members lying in a region with a radius of  $\sim 100h^{-1}$  kpc. Additionally, there is not a clear separation between the positive velocity galaxies and the negative velocity galaxies (see Figure 3b), indicating that the bimodality of the velocity distribution for the foreground group might be a result of incomplete sampling.

## 5. LENS MODELS

There are several ways to apply the group environments to the lensing models of B2319 and B1600. One method is to treat the group as a single dark matter halo and model the group as a smooth mass distribution. Alternatively, we could model each of the group members individually. This allows the possibility that our groups might be chance associations of galaxies instead of bound systems. Finally, we may model the group as lumpy masses embedded in a smooth distribution, a combination of the former two cases. This model of a halo with substructure is consistent with cluster observations and theoretical predictions (Natarajan & Springel 2004; Gao et al. 2004; Zentner et al. 2005). However, due to incomplete information about our groups, in this analysis we only use the first two methods to give approximate indications for the contributions of the group environments to the lenses. For simplicity, we model all halos as singular isothermal spheres (SIS).

### 5.1. B2319 Lens Models

Models for B2319 were found to inadequately reproduce the image configuration without applying a large shear term ( $\gamma = 0.14, \text{PA}_\gamma = -22^\circ$ ; Rusin et al. 2001). The necessary additional shear is essentially perpendicular to the expected orientation of the shear caused by the lensing galaxy, and this excess shear is therefore assumed to be caused by another object. We investigate whether the foreground and background groups we have detected can adequately account for this discrepancy. Although

the groups associated with B2319 are not at the same redshift as the primary lensing galaxy, we calculate the shear at the lensing plane of the groups and identify this as the same shear required by Rusin et al. (2001) (see also Fassnacht et al. 2005; Momcheva et al. 2005).

We create two models for the system by accounting for the foreground and background groups and for the individual galaxies of both groups. The groups and the individual galaxies are all modeled with SIS profiles, where the brightest galaxy in each group is assigned a fiducial velocity dispersion of  $\sigma = 200 \text{ km s}^{-1}$  and the contributions of the other galaxies are scaled by  $10^{-0.2(m-m_{fid})}$  where  $m_{fid}$  is the magnitude of the brightest galaxy (e.g., Keeton & Zabludoff 2004; Fassnacht et al. 2005). For the group model, we use the luminosity-weighted average position of the group galaxies to determine the group centroid. The results for these models are collected in Table 7. We find a total additional shear of  $\gamma = 0.05$  at a PA of  $33^\circ$  for the group halo model and a shear of  $\gamma = 0.023$  at a PA of  $86^\circ$  for the individual galaxies model. This correction differs substantially from the shear required by Rusin et al. (2001) in both magnitude and orientation, although this could be caused by our uncertainty in the true position of the group centroid.

### 5.2. B1600 Lens Models

The model for B1600+434 adequately reproduces the observed image distribution with physically reasonable parameters (Koopmans et al. 1998). However, the presence of the group that includes the lensing galaxy adds an additional mass sheet to the lens plane. This mass sheet increases the convergence in the lens model, which in turn effects the value of  $H_0$  determined for this lens system. The additional convergence will decrease the value of  $H_0$  compared to models that do not account for the lens environment:

$$H_{0,true} = H_{0,meas} (1 - \kappa_{group}).$$

In this analysis, we calculate the expected added convergence due to the group, due to the individual galaxies excluding the lensing galaxy, and due to the individual galaxies excluding the lens and its neighbor galaxy. The neighbor galaxy has already been included in some lens models (see Maller et al. 2000, for example). We use the luminosity-weighted positions of the group members to determine the group centroid for the group SIS. Results for each of the models are collected in Table 8. Previous analyses of B1600 have derived values of  $H_0$  between  $52 \text{ km s}^{-1} \text{ Mpc}^{-1}$  and  $60 \text{ km s}^{-1} \text{ Mpc}^{-1}$  (Burud et al. 2000; Koopmans et al. 2000), already lower than values determined by other methods (e.g., Sánchez et al. 2006; Tegmark et al. 2004; Freedman et al. 2001). The additional convergence due to the environment of B1600 lowers these values by a further  $\sim 5\%$ .

## 6. DISCUSSION AND CONCLUSIONS

The absence of early-type galaxies and X-ray emission indicates that the B1600 group may not be a relaxed or bound system. Furthermore, the elongated structure of the group may favor this unrelaxed interpretation, although groups have been shown to have a wide range of morphologies (Zabludoff & Mulchaey 1998; Wilman et al. 2005a). Though our sampling is not complete enough to make strong statements regarding the

TABLE 7  
B2319 LENS ENVIRONMENT MODELING

Model	$\kappa_{frg}$	$\gamma_{frg}$	$PA_{frg}$	$\kappa_{bkg}$	$\gamma_{bkg}$	$PA_{bkg}$	$\kappa_{total}$	$\gamma_{total}$	$PA_{total}$
Groups	0.046	0.046	37	0.006	0.006	-7	0.051	0.050	33
Individual Galaxies	0.033	0.025	100	0.008	0.006	-14	0.041	0.023	86

NOTE. — Values marked *frg* are for the foreground group, those marked *bkg* are for the background group, and those marked *total* are for the sum of the contributions of the foreground and background groups.

TABLE 8  
B1600 LENS ENVIRONMENT MODELING

Model	$\kappa_{env}$	$\gamma_{env}$	$PA_{env}$
Group	0.014	0.014	18
Individual galaxies <sup>a</sup>	0.050	0.031	-53
Individual galaxies <sup>b</sup>	0.012	0.008	98

<sup>a</sup>Excluding the lensing galaxy

<sup>b</sup>Excluding the lensing galaxy and its neighbor

characteristic length and mass scales for this group, we find the mass to be consistent with other groups with similar membership (e.g., Zabludoff & Mulchaey 1998; Ramella et al. 1989). However, the arguments for and against the bound interpretation of these galaxies all rely on comparisons with local groups. It seems perfectly reasonable to expect that groups at higher redshifts are dynamically younger and therefore their constituent galaxies have not had time to undergo processing. This would account for the absence of early-type galaxies and hot intragroup gas. The compactness of the distribution of the central members of the group and the presence of a strong gravitational lens are indicators that, at a minimum, the *central structure* of the group is bound in a common halo, and we therefore conclude that B1600 lies in a group environment.

The groups associated with B2319 are similar to groups found in the local Universe; the numbers of members, early-type fractions, and velocity dispersions of these two groups are typical of local groups. The foreground group is potentially a poor cluster, and is a good candidate for X-ray followup (e.g., Jeltama et al. 2006). The nature of the background group is more difficult to discern; the group has an irregular morphology with no proper core but a large early-type fraction. The absence of a core might portend a group that is forming, though the large early-type fraction suggests the constituent galaxies have had several significant interactions. It is worth noting that we did not target galaxies at a redshift of  $z \sim 0.7$ , and more complete spectroscopy of the field might make a core structure more apparent for the group. In any case, the number of members (8) and the approximately gaussian nature of the velocity histogram for this group (Figure 3c) give us confidence that this is a group associated with a common halo.

Accounting for the environments of gravitational lenses in the model of the potential is theoretically straightforward but quite difficult to do in practice. The lens corrections based upon individual galaxies rely on incomplete membership information and incorrect mod-

eling of velocity dispersions for individual group members. These problems are probably less severe than those present for the group halo model. Velocity dispersion estimates for group halos can be off by significant amounts because of incomplete group membership sampling (Zabludoff & Mulchaey 1998). Due to the quadratic dependence of SIS models on velocity dispersions, modeling errors for SIS models can be substantial for poorly sampled groups. Another important source of error is the modeling of centroids for the groups. Different centroiding methods can yield very different angular offsets of the group from the lens due to sampling small numbers of the group members (e.g., Fassnacht & Lubin 2002; Fassnacht et al. 2005). Additionally, the SIS model assumes a relaxed group halo, though this might not be the case for many moderate redshift groups (see the discussion of the B1600 group above).

Deep X-ray observations of lens systems would potentially correct for all of the problems associated with modeling group halos; the presence of diffuse X-ray emission would indicate the presence of a group halo, the X-ray temperature could be used as a mass measure, and the diffuse X-ray centroid would presumably coincide with the mass centroid (Mulchaey et al. 2003). However, for all but the most massive groups, it is very difficult to detect intragroup X-ray emission due to the low luminosities and cosmological dimming of these moderate redshift sources (Dai & Kochanek 2005; Neureuther et al. 2006, *in prep*), although some detections have been made (Jeltama et al. 2006; Mulchaey et al. 2006; Grant et al. 2004). Thus, for our groups with only optical information, we favor using the individual galaxies to interpret our results as lower bounds on lens corrections due to group environments.

We find that the environments for each lens system contribute approximately 5% to the convergence in the lensing models, as shown in Tables 7 and 8, similar to results obtained by Momcheva et al. (2005). For B1600, this suggests a commensurate 5% decrease in the determined value of  $H_0$ . Note that ignoring lens environments

causes a *systematically* inflated value of  $H_0$ , and our analysis simply removes (some of) this bias; this should be considered a reinterpretation of the previously published values of  $H_0$  for this lens system and not a new calculation for the Hubble Constant. We also find that the environment adds a small contribution to the shear, although we emphasize that this is *very* dependent on the membership determined for the groups. However, we targeted most reasonable candidates within  $\sim 10''$  of the lenses, leading us to believe that we have complete membership information for galaxies that would most significantly affect the lensing. We are in the process of investigating several more lens systems and we will attempt to quantify uncertainties in our convergence and shear estimates based upon this larger sample.

Based in part on observations made with the NASA/ESA Hubble Space Telescope, obtained from the the Data Archive at the Space Telescope Science Institute (STScI). STScI is operated by the Association

of Universities for Research in Astronomy, Inc., under NASA contract NAS5-26555. These observations are associated with program #AR-10300, supported by NASA through a grant from STScI. Additionally, some of the data presented herein were obtained at the W.M. Keck Observatory, which is operated as a scientific partnership among the California Institute of Technology, the University of California and the National Aeronautics and Space Administration. The Observatory was made possible by the generous financial support of the W.M. Keck Foundation. The authors wish to recognize and acknowledge the very significant cultural role and reverence that the summit of Mauna Kea has always had within the indigenous Hawaiian community. We are most fortunate to have the opportunity to conduct observations from this mountain. This work is also based in part on data collected at the Subaru Telescope and obtained from the SMOKA science archive at the Astronomical Data Analysis Center, which are operated by the National Astronomical Observatory of Japan.

## REFERENCES

- Aarseth, S. J., & Fall, S. M. 1980, *ApJ*, 236, 43  
 Abazajian, K., et al. 2005, *ApJ*, 625, 613  
 Aceves, H., & Velázquez, H. 2002, *Revista Mexicana de Astronomía y Astrofísica*, 38, 199  
 Baba, H., et al. 2002, *ASP Conf. Ser.* 281: *Astronomical Data Analysis Software and Systems XI*, 281, 298  
 Bahcall, J. N., Kirhakos, S., Saxe, D. H., & Schneider, D. P. 1997, *ApJ*, 479, 642  
 Balogh, M., et al. 2004, *MNRAS*, 348, 1355  
 Best, P. N. 2004, *MNRAS*, 351, 70  
 Best, P. N., Kauffmann, G., Heckman, T. M., Brinchmann, J., Charlot, S., Ivezić, Ž., & White, S. D. M. 2005, *MNRAS*, 660  
 Blandford, R., Surpi, G., & Kundić, T. 2001, *ASP Conf. Ser.* 237: *Gravitational Lensing: Recent Progress and Future Goals*, 237, 65  
 Bower, R. G., & Balogh, M. L. 2004, *Clusters of Galaxies: Probes of Cosmological Structure and Galaxy Evolution*, 326  
 Browne, I. W. A., et al. 2003, *MNRAS*, 341, 13  
 Burud, I., et al. 2000, *ApJ*, 544, 117  
 Carlberg, R. G., Yee, H. K. C., Morris, S. L., Lin, H., Hall, P. B., Patton, D. R., Sawicki, M., & Shepherd, C. W. 2001, *ApJ*, 552, 427  
 Carlberg, R. G., Yee, H. K. C., Morris, S. L., Lin, H., Hall, P. B., Patton, D. R., Sawicki, M., & Shepherd, C. W. 2001, *ApJ*, 563, 736  
 Chae, K.-H., Mao, S., & Augusto, P. 2001, *MNRAS*, 326, 1015  
 Coil, A. L., et al. 2004, *ApJ*, 609, 525  
 Coil, A. L., et al. 2006, *ApJ*, 638, 668  
 Colless, M., et al. 2001, *MNRAS*, 328, 1039  
 Collister, A. A., & Lahav, O. 2005, *MNRAS*, 361, 415  
 Conselice, C. J., Bershad, M. A., Dickinson, M., & Papovich, C. 2003, *AJ*, 126, 1183  
 Dai, X., & Kochanek, C. S. 2005, *ApJ*, 625, 633  
 Dalal, N., & Watson, C. R. 2004, *ArXiv Astrophysics e-prints*, arXiv:astro-ph/0409483  
 D’Onghia, E., & Lake, G. 2004, *ApJ*, 612, 628  
 Evrard, A. E., et al. 2002, *ApJ*, 573, 7  
 Fassnacht, C. D., & Cohen, J. G. 1998, *AJ*, 115, 377  
 Fassnacht, C. D., & Lubin, L. M. 2002, *AJ*, 123, 627  
 Fassnacht, C. D., Gal, R. R., Lubin, L. M., McKean, J. P., Squires, G. K., & Readhead, A. C. S. 2006, *ApJ*, in press (astro-ph/0510728)  
 Faure, C., Alloin, D., Kneib, J. P., & Courbin, F. 2004, *A&A*, 428, 741  
 Freedman, W. L., et al. 2001, *ApJ*, 553, 47  
 Gao, L., White, S. D. M., Jenkins, A., Stoehr, F., & Springel, V. 2004, *MNRAS*, 355, 819  
 Gerke, B. F., et al. 2005, *ApJ*, 625, 6  
 Gómez, P. L., et al. 2003, *ApJ*, 584, 210  
 Grant, C. E., Bautz, M. W., Chartas, G., & Garmire, G. P. 2004, *ApJ*, 610, 686  
 Hickson, P. 1982, *ApJ*, 255, 382  
 Hoekstra, H., et al. 2001, *ApJ*, 548, L5  
 Jackson, N., et al. 1995, *MNRAS*, 274, L25  
 Jeltama, T. E., Mulchaey, J. S., Lubin, L. M., Rosati, P., Böhringer, H. 2006, *ApJ*, submitted  
 Kauffmann, G., White, S. D. M., Heckman, T. M., Ménard, B., Brinchmann, J., Charlot, S., Tremonti, C., & Brinkmann, J. 2004, *MNRAS*, 353, 713  
 Keeton, C. R., Christlein, D., & Zabludoff, A. I. 2000, *ApJ*, 545, 129  
 Keeton, C. R., & Zabludoff, A. I. 2004, *ApJ*, 612, 660  
 Kochanek, C. S. 2002, *ApJ*, 578, 25  
 Kochanek, C. S. 2003, *ApJ*, 583, 49  
 Kochanek, C. S., & Schechter, P. L. 2004, *Measuring and Modeling the Universe*, 117  
 Koopmans, L. V. E., de Bruyn, A. G., & Jackson, N. 1998, *MNRAS*, 295, 534  
 Koopmans, L. V. E., de Bruyn, A. G., Xanthopoulos, E., & Fassnacht, C. D. 2000, *A&A*, 356, 391  
 Koopmans, L. V. E., Treu, T., Fassnacht, C. D., Blandford, R. D., & Surpi, G. 2003, *ApJ*, 599, 70  
 Lehar, J., et al. 2000, *ApJ*, 536, 584  
 Lin, L., et al. 2004, *ApJ*, 617, L9  
 Lubin, L. M., Fassnacht, C. D., Readhead, A. C. S., Blandford, R. D., & Kundić, T. 2000, *AJ*, 119, 451  
 Maller, A. H., Simard, L., Guhathakurta, P., Hjorth, J., Jaunsen, A. O., Flores, R. A., & Primack, J. R. 2000, *ApJ*, 533, 194  
 McLure, R. J., & Dunlop, J. S. 2001, *MNRAS*, 321, 515  
 Merchán, M. E., & Zandivarez, A. 2005, *ApJ*, 630, 759  
 Miller, C. J., Nichol, R. C., Gómez, P. L., Hopkins, A. M., & Bernardi, M. 2003, *ApJ*, 597, 142  
 Miyazaki, S., et al. 2002, *PASJ*, 54, 833  
 Möller, O., Natarajan, P., Kneib, J.-P., & Blain, A. W. 2002, *ApJ*, 573, 562  
 Momcheva, I., Williams, K. A., Keeton, C. R., & Zabludoff, A. I. 2005, *ArXiv Astrophysics e-prints*, arXiv:astro-ph/0511594  
 Morgan, N. D., Kochanek, C. S., Pevunova, O., & Schechter, P. L. 2005, *AJ*, 129, 2531  
 Mulchaey, J. S., Davis, D. S., Mushotzky, R. F., & Burstein, D. 2003, *ApJS*, 145, 39  
 Mulchaey, J. S., Lubin, L. M., Fassnacht, C. D., Rosati, P., & Jeltama, T. E. 2006, *ApJ*, submitted  
 Myers, S. T., et al. 2003, *MNRAS*, 341, 1  
 Natarajan, P., & Springel, V. 2004, *ApJ*, 617, L13  
 Oguri, M., Keeton, C. R., & Dalal, N. 2005, *MNRAS*, 364, 1451  
 Ouchi, M., et al. 2004, *ApJ*, 611, 660  
 Oke, J. B., et al. 1995, *PASP*, 107, 375  
 Padilla, N. D., et al. 2004, *MNRAS*, 352, 211

- Patton, D. R., et al. 2002, *ApJ*, 565, 208
- Ramella, M., Geller, M. J., & Huchra, J. P. 1989, *ApJ*, 344, 57
- Reed, D., Governato, F., Quinn, T., Gardner, J., Stadel, J., & Lake, G. 2005, *MNRAS*, 359, 1537
- Rusin, D., et al. 2001, *AJ*, 122, 591
- Sánchez, A. G., Baugh, C. M., Percival, W. J., Peacock, J. A., Padilla, N. D., Cole, S., Frenk, C. S., & Norberg, P. 2006, *MNRAS*, 366, 189
- Sheinis, A. I., Bolte, M., Epps, H. W., Kibrick, R. I., Miller, J. S., Radovan, M. V., Bigelow, B. C., & Sutin, B. M. 2002, *PASP*, 114, 851
- Tanaka, M., Goto, T., Okamura, S., Shimasaku, K., & Brinkmann, J. 2004, *AJ*, 128, 2677
- Tegmark, M., et al. 2004, *Phys. Rev. D*, 69, 103501
- Tully, R. B. 1987, *ApJ*, 321, 280
- Weinmann, S. M., van den Bosch, F. C., Yang, X., & Mo, H. J. 2006, *MNRAS*, 366, 2
- Williams, K. A., Momcheva, I., Keeton, C. R., Zabludoff, A. I., & Lehar, J. 2005, *ArXiv Astrophysics e-prints*, arXiv:astro-ph/0511593
- Wilman, D. J., Balogh, M. L., Bower, R. G., Mulchaey, J. S., Oemler, A., Carlberg, R. G., Morris, S. L., & Whitaker, R. J. 2005a, *MNRAS*, 358, 71
- Wilman, D. J., et al. 2005b, *MNRAS*, 358, 88
- Yang, X., Mo, H. J., Jing, Y. P., van den Bosch, F. C., & Chu, Y. 2004, *MNRAS*, 350, 1153
- York, D. G., et al. 2000, *AJ*, 120, 1579
- Zabludoff, A. I., & Mulchaey, J. S. 1998, *ApJ*, 496, 39
- Zentner, A. R., Berlind, A. A., Bullock, J. S., Kravtsov, A. V., & Wechsler, R. H. 2005, *ApJ*, 624, 505